

# Water-Mediated Carbon–Oxygen Hydrogen Bonding Facilitates S-Adenosylmethionine Recognition in the Reactivation Domain of Cobalamin-Dependent Methionine Synthase

Robert J. Fick,<sup>†</sup> Mary C. Clay,<sup>‡</sup> Lucas Vander Lee,<sup>†</sup> Steve Scheiner,<sup>§</sup> Hashim Al-Hashimi,<sup>‡</sup> and Raymond C. Trievel<sup>\*,†</sup>

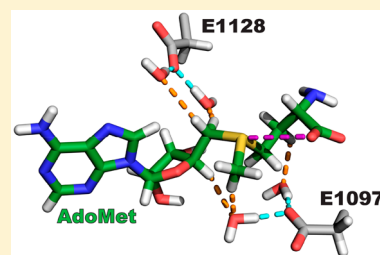
<sup>†</sup>Department of Biological Chemistry, University of Michigan, Ann Arbor, Michigan 48109, United States

<sup>‡</sup>Department of Biochemistry, Duke University, Durham, North Carolina 27710, United States

<sup>§</sup>Department of Chemistry and Biochemistry, Utah State University, Logan, Utah 84322, United States

**S** Supporting Information

**ABSTRACT:** The C-terminal domain of cobalamin-dependent methionine synthase (MetH) has an essential role in catalyzing the reactivation of the enzyme following the oxidation of its cobalamin cofactor. This reactivation occurs through reductive methylation of the cobalamin using S-adenosylmethionine (AdoMet) as the methyl donor. Herein, we examine the molecular recognition of AdoMet by the MetH reactivation domain utilizing structural, biochemical, and computational approaches. Crystal structures of the *Escherichia coli* MetH reactivation domain in complex with AdoMet, the methyl transfer product S-adenosylhomocysteine (AdoHcy), and the AdoMet analogue inhibitor sinefungin illustrate that the ligands exhibit an analogous conformation within the solvent-exposed substrate binding cleft of the enzyme. AdoMet binding is stabilized by an intramolecular sulfur–oxygen chalcogen bond between the sulfonium and carboxylate groups of the substrate and by water-mediated carbon–oxygen hydrogen bonding between the sulfonium cation and the side chains of Glu1097 and Glu1128 that bracket the substrate binding cleft. AdoMet and sinefungin exhibited similar binding affinities for the MetH reactivation domain, whereas AdoHcy displayed an affinity for the enzyme that was an order of magnitude lower. Mutations of Glu1097 and Glu1128 diminished the AdoMet/AdoHcy binding selectivity ratio to approximately 2-fold, underscoring the role of these residues in enabling the enzyme to discriminate between the substrate and product. Together, these findings indicate that Glu1097 and Glu1128 in MetH promote high-affinity recognition of AdoMet and that sinefungin and potentially other AdoMet-based methyltransferase inhibitors can abrogate MetH reactivation, which would result in off-target effects associated with alterations in methionine homeostasis and one-carbon metabolism.



Cobalamin-dependent methionine synthase (MetH) is a dynamic multidomain enzyme that plays a central role in one-carbon metabolism by catalyzing the methylation of homocysteine to methionine using methyltetrahydrofolate ( $\text{CH}_3\text{-H}_4\text{folate}$ ). In MetH, this reaction occurs through the transfer of a methyl group from  $\text{CH}_3\text{-H}_4\text{folate}$  to cob(I)alamin [ $\text{Co(I)Cbl}$ ] to form  $\text{CH}_3\text{-Co(III)Cbl}$ , which subsequently methylates homocysteine to yield methionine.<sup>1–3</sup> During turnover under aerobic conditions,  $\text{Co(I)Cbl}$  is oxidized to  $\text{Co(II)Cbl}$  every  $\sim 2000$  reactions, inactivating the enzyme.<sup>4</sup> MetH activity is restored through a one-electron reduction of  $\text{Co(II)Cbl}$  to  $\text{Co(I)Cbl}$  by MetH reductase, coupled with S-adenosylmethionine (AdoMet)-dependent methylation of the coenzyme by the C-terminal reactivation domain of MetH. The methionine generated by MetH is utilized in protein synthesis and the biosynthesis of AdoMet, the predominant methyl donor utilized in metabolic pathways, cellular signaling, and gene regulation. Thus, the reactivation domain of MetH plays an essential role in maintaining methyl homeostasis in biological systems.

Biochemical and structural studies have provided important insights into the mechanism of reactivation of MetH by its C-terminal domain. Initial structural characterization of the *Escherichia coli* MetH reactivation domain by Dixon et al. revealed that it adopts a crescent-shaped fold that is unique from other classes of AdoMet-dependent methyltransferases, leading to its categorization as a class II methyltransferase.<sup>5,6</sup> AdoMet binds in a relatively solvent-exposed cleft in the concave face of the domain. Two glutamate residues, Glu1097 and Glu1128, flank the AdoMet binding site but do not directly interact with the substrate. However, the proximity of these two glutamates to AdoMet was proposed to promote substrate recognition through electrostatic interactions with the substrate's sulfonium cation. Subsequent structural and functional studies of MetH have demonstrated that the exposed AdoMet binding cleft in the reactivation domain permits the substrate to dock with the large planar corrin ring system in the cobalamin

Received: April 2, 2018

Revised: May 4, 2018

Published: May 7, 2018

66 binding domain, facilitating methylation of the cofactor during  
67 enzyme reactivation.<sup>7–9</sup>

68 A recent survey of representative high-resolution crystal  
69 structures from several classes of AdoMet-dependent methyl-  
70 transferases has revealed the widespread presence of carbon–  
71 oxygen (CH...O) hydrogen bonds between the AdoMet methyl  
72 group and oxygen atoms with the enzymes' active sites.<sup>10</sup> These  
73 interactions have been shown to be important in high-affinity  
74 AdoMet recognition and for promoting catalysis in the SET  
75 domain class of lysine methyltransferases. Interestingly, the  
76 structure of the MetH reactivation domain bound to AdoMet  
77 does not exhibit direct CH...O hydrogen bonding between the  
78 AdoMet methyl group and the enzyme, in contrast to the case  
79 for other classes of methyltransferases. This observation  
80 spurred us to examine whether other interactions with the  
81 active site are important in conferring substrate specificity in  
82 MetH.

## 83 ■ EXPERIMENTAL PROCEDURES

84 **Reagents.** S-Adenosylhomocysteine and sinefungin were  
85 purchased from Millipore-Sigma. S-Adenosylmethionine *p*-  
86 toluenesulfonate was purchased from Carbosynth and purified  
87 by ion-exchange chromatography.<sup>11</sup> <sup>13</sup>CH<sub>3</sub>-AdoMet was  
88 enzymatically synthesized using *E. coli* AdoMet synthetase  
89 with methyl-<sup>13</sup>C-methionine (Cambridge Isotope Laboratories)  
90 and adenosine triphosphate and purified as previously  
91 described.<sup>11</sup>

92 **Protein Expression and Purification.** The cDNA  
93 encoding the C-terminal domain of *E. coli* MetH (residues  
94 897–1227; UniProt entry P13009) was cloned into a variant of  
95 pET15b with a tobacco etch virus (TEV) protease-cleavable N-  
96 terminal hexahistidine tag. The E1097Q and E1128Q  
97 mutations were prepared using QuikChange mutagenesis  
98 (Agilent) and confirmed using dideoxy sequencing. Expression  
99 vectors were transformed into *E. coli* Rosetta2 DE3 cells  
100 (Novagen) cultured in 2XYT medium, and protein expression  
101 was induced at 18 °C overnight. The wild-type (WT) MetH  
102 reactivation domain and glutamine mutants were purified using  
103 a combination of Co(II) Talon affinity and Superdex 200 gel  
104 filtration chromatography (GE Healthcare). Prior to gel  
105 filtration purification, the protein was incubated with charcoal  
106 to remove AdoMet that co-purified with the enzyme, as  
107 previously described.<sup>12</sup> The purified proteins were concen-  
108 trated, flash-frozen in liquid nitrogen, and stored at –80 °C.  
109 Protein concentrations were determined by their absorbance at  
110 280 nm.

111 **Crystallization and Structure Determination.** The  
112 MetH reactivation domain was crystallized using the hanging  
113 drop method in 60–100 mM TRIS (pH 7.2–7.5), 300 mM  
114 magnesium acetate, and 27–32% PEG 6000, similar to the  
115 previously reported crystallization conditions.<sup>5</sup> The protein  
116 solution contained 15 mg/mL MetH, 10 mM TRIS (pH 7.4),  
117 10 mM EDTA, and 3.0 mM AdoMet, 3.0 mM sinefungin, or  
118 5.0 mM AdoHcy. X-ray diffraction data were collected at Life  
119 Sciences Collaborative Access Team beamline 21-ID-G at the  
120 Advanced Photon Source Synchrotron at Argonne National  
121 Laboratory and were processed using HKL2000.<sup>13</sup> Structures of  
122 the MetH complexes were determined by molecular replace-  
123 ment using Phaser with the coordinates of the *E. coli* MetH  
124 reactivation domain [Protein Data Bank (PDB) entry 1MSK]  
125 as the search model.<sup>14</sup> Model building, refinement, and  
126 validation were performed using Coot and Phenix.<sup>15–17</sup>  
127 Structural figures were rendered using PyMOL (Schrödinger,

128 LLC), and electrostatic surface calculations were performed  
129 using the APBS plugin for PyMOL.<sup>18</sup>

**Isothermal Titration Calorimetry (ITC).** ITC was 130  
performed using a MicroCal VP-ITC calorimeter (Malvern 131  
Instruments) for WT MetH and a MicroCal Auto-iTC200 132  
instrument (Malvern Instruments) for the MetH E1097Q and 133  
E1128Q mutants. Titrations were performed using 20 mM 134  
sodium phosphate (pH 8.0) and 100 mM sodium chloride. 135  
Experiments with the WT enzyme and AdoMet or sinefungin 136  
were performed with 60 μM protein and 600 μM ligand, 137  
whereas the AdoHcy titrations were performed with 200 μM 138  
protein and 2.2 mM ligand. Experiments using the E1097Q and 139  
E1128Q mutants utilized 830–940 μM protein and 9.6 mM 140  
AdoMet, 16.1 mM sinefungin, or 10.1–10.7 mM AdoHcy. The 141  
sinefungin titrations with the MetH mutants required a higher 142  
ligand concentration. Control titrations of sinefungin at these 143  
higher concentrations, which approached the concentration of 144  
the phosphate buffer, exhibited a significant background heat, 145  
potentially because of titration of the amine group in 146  
sinefungin. To correct for this effect, sinefungin was dissolved 147  
in buffer and the solution was adjusted to pH 8.0 using 200 148  
mM HCl in 20 mM sodium phosphate and 100 mM sodium 149  
chloride (final concentration) to maintain the phosphate and 150  
sodium ion concentrations. Data were processed using Origin 151  
(OriginLab Corp.). Stoichiometries of binding (*N* values) 152  
ranged from 0.9 to 1.1. 153

**Nuclear Magnetic Resonance (NMR) Spectroscopy.** All 154  
NMR experiments were performed on a Bruker Avance III 600 155  
MHz spectrometer equipped with a 5 mm triple-resonance 156  
cryogenic probe. Spectra were recorded at 25 °C using 0.2 mM 157  
<sup>13</sup>CH<sub>3</sub>-AdoMet in 20 mM sodium phosphate, 100 mM NaCl, 158  
and 10% D<sub>2</sub>O at pH 7.0 (SET7/9) or pH 8.0 (MetH) and 159  
referenced relative to the water signal. Data were processed and 160  
analyzed using NMRPipe and Sparky, respectively.<sup>19,20</sup> The 161  
enzyme-bound chemical shift was determined using <sup>1</sup>H–<sup>13</sup>C 162  
heteronuclear single-quantum correlation (HSQC) spectra of 163  
<sup>13</sup>C-methyl-labeled AdoMet recorded in the presence and 164  
absence of a 1.2-fold molar stoichiometric excess of SET7/9 or 165  
MetH (0.24 mM). <sup>1</sup>H–<sup>13</sup>C band-selective optimized flip angle 166  
short transient heteronuclear multiple-quantum correlation 167  
(SOFAST-HMQC) spectra were also recorded to assess the 168  
relative solvent accessibility of the enzyme-bound AdoMet. 169

**Quantum Mechanics (QM) Calculations.** All quantum 170  
calculations were performed within the framework of the 171  
Gaussian-09 set of codes.<sup>21</sup> The 6-31+G\*\* basis set was applied 172  
at the DFT level, using the M06-2X functional.<sup>22</sup> Geometries 173  
were fully optimized under the restriction that certain atoms 174  
were held in their crystallographic coordinates. Optimizations 175  
were performed in an aqueous solvent, using the CPCM 176  
variant<sup>23</sup> of self-consistent reaction field theory. The binding 177  
energy, *E<sub>B</sub>*, of each complex was evaluated in vacuo as the 178  
difference between the energy of the entire complex and the 179  
sum of the energies of (a) the MeS<sup>+</sup>(Et)<sub>2</sub> and S(Et)<sub>2</sub> 180  
monomers, representing AdoMet and AdoHcy, respectively, 181  
and (b) the propionate and propionamide group and their 182  
cognate water molecules, mimicking Glu1097 and Glu1128 and 183  
their corresponding glutamine mutations with the water 184  
molecules bridging to the ligands. 185

## 186 ■ RESULTS

To gain molecular insights into its substrate specificity, we 187  
determined high-resolution crystal structures of the *E. coli* 188

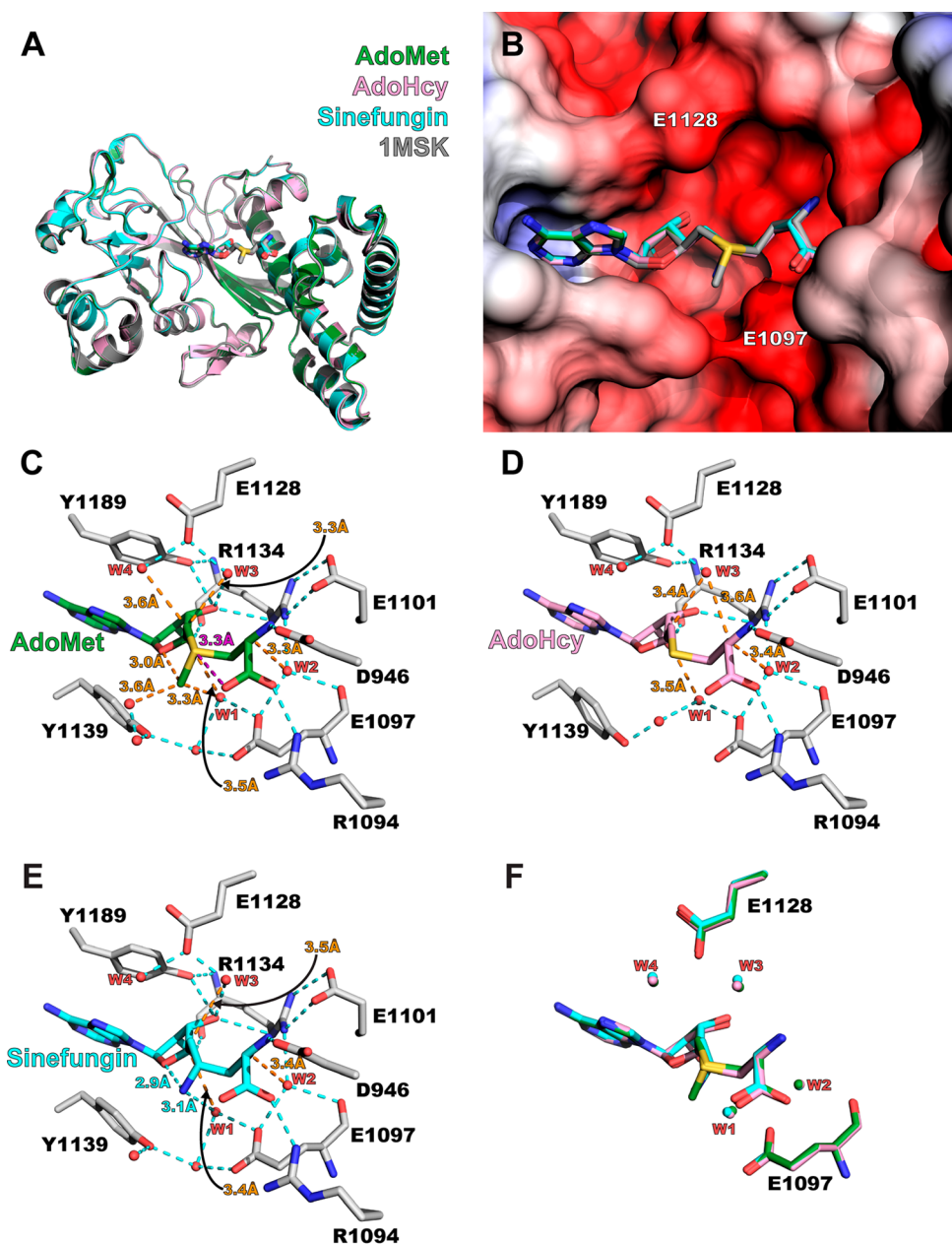


**Figure 1.** Crystal structures of the MetH complexes. (A) Superimposition of the MetH complexes of AdoMet (green), AdoHcy (pink), sinefungin (cyan), and the previously determined MetH·AdoMet complex (PDB entry 1MSK, gray). (B) Electrostatic surface of the substrate binding cleft with AdoMet, sinefungin, and AdoHcy aligned based on the superimposition from panel A. The electrostatic potential is contoured from  $-5.0$  to  $5.0$  kT/e with red and blue denoting acidic and basic surfaces, respectively. The positions of Glu1097 and -1128 are labeled, and the ligands are colored according to the scheme used in panel A. Structures of the MetH substrate binding cleft bound to (C) AdoMet, (D) AdoHcy, and (E) sinefungin. Conventional hydrogen bonds are depicted by cyan dashes, whereas  $\text{CH}\cdots\text{O}$  hydrogen bonds are denoted as orange dashes. Distances for the hydrogen bonds formed by the four water molecules (W1–W4) that mediate interactions between the ligands and Glu1097 and Glu1128 are illustrated. (F) Structural overlay of ligands, Glu1097, Glu1128, and the four water molecules in the AdoMet, AdoHcy, and sinefungin complexes from the superimposition in panel A. The water molecules and glutamate side chains are colored according to their corresponding ligand.

189 MetH reactivation domain bound to AdoMet, AdoHcy, and the  
 190 AdoMet analogue inhibitor sinefungin (Table S1). The  
 191 modeling of the ligands in the structures was verified using  
 192 simulated annealing omit maps (Figure S1). Superimposition of  
 193 the reactivation domain complexes and the previously reported  
 194 structure of the MetH·AdoMet complex illustrates their high  
 195 degree of structural similarity, with root-mean-square deviations  
 196 for the aligned  $\text{C}\alpha$  atoms of  $\leq 0.32$  Å (Figure 1A). In addition,  
 197 the structural alignment of the complexes reveals that AdoMet,  
 198 AdoHcy, and sinefungin adopt nearly identical conformations

when bound in the enzyme's solvent-exposed substrate binding  
 199 cleft (Figure 1B). This conformation is distinct from the  
 200 AdoMet binding modes observed in other classes of  
 201 methyltransferases and is stabilized in part by an intramolecular  
 202  $\text{S}\cdots\text{O}$  chalcogen bond between carboxylate and sulfonium ions  
 203 in the substrate (Figure 1C), analogous to the chalcogen bond  
 204 formed by AdoMet and an asparagine in the lysine  
 205 methyltransferase SET7/9.<sup>12</sup> In addition, the AdoMet methyl  
 206 group and the ether O4 atom in the ribose ring are oriented in  
 207 a geometry consistent with an intramolecular  $\text{CH}\cdots\text{O}$  hydrogen  
 208

209 bond. In addition to these intramolecular interactions, an  
 210 extensive network of direct and water-mediated hydrogen  
 211 bonds and van der Waals interactions between AdoMet and the  
 212 residues composing the binding pocket in the enzyme facilitate  
 213 substrate recognition. An examination of the AdoHcy and  
 214 sinefungin complexes reveals an analogous network of  
 215 intermolecular interactions that promote binding of the enzyme  
 216 to the product and inhibitor, respectively (Figure 1D,E).  
 217 Correlatively, superimposition of the three MetH complexes  
 218 illustrates an analogous conformation adopted by AdoMet,  
 219 AdoHcy, and sinefungin (Figure 1F).

220 Given the similarity in the ligands' binding modes and their  
 221 interactions with MetH reactivation domain, we sought to  
 222 understand the determinants that confer selectivity in AdoMet  
 223 recognition. Initial structural studies of the reactivation domain  
 224 by Dixon et al. suggested Glu1097 and Glu1128 as being  
 225 important to AdoMet binding (Figure 1C).<sup>5</sup> The side chains of  
 226 these residues are within 6 Å of the sulfur cation of the  
 227 substrate but do not participate in direct interactions with the  
 228 sulfonium group. They proposed that electrostatic interaction  
 229 between the carboxylate groups of Glu1097 and Glu1128 and  
 230 the AdoMet sulfonium cation would favor binding of the  
 231 substrate compared to the product AdoHcy in which the  
 232 sulfonium is replaced by a neutral thioether moiety. Consistent  
 233 with this observation, electrostatic surface calculations of the  
 234 MetH reactivation domain illustrate that the substrate binding  
 235 cleft is relatively acidic, conducive to the recognition of the  
 236 AdoMet sulfonium cation (Figure 1B).

237 A close inspection of the substrate binding cleft reveals two  
 238 pairs of water molecules that mediate hydrogen bonding  
 239 between AdoMet and Glu1097 and Glu1128. For the sake of  
 240 clarity, we have termed these water molecules W1–W4. W1  
 241 facilitates CH···O hydrogen bonding between the Glu1097  
 242 carboxylate group and the AdoMet methyl group and the C4  
 243 atom in the ribose ring, whereas W2 serves to bridge hydrogen  
 244 bonding between Glu1097 and the C $\beta$  methylene group of the  
 245 substrate (Figure 1C). The C $\beta$  and C4 atoms in AdoMet are  
 246 one carbon atom removed from the sulfur cation but remain  
 247 partially polarized because of their proximity to the cation and  
 248 can participate in CH···O hydrogen bonding, albeit more  
 249 weakly than a carbon atom bonded directly to the sulfur  
 250 cation.<sup>24</sup> W3 and W4 form a CH···O hydrogen bonding bridge  
 251 between the Glu1128 carboxylate anion and the C5 methylene  
 252 group in the substrate. In addition, W3 forms an OH···O  
 253 hydrogen bond to the 3'-hydroxyl group of the ribose ring of  
 254 AdoMet. A superimposition of the structures of the AdoMet,  
 255 AdoHcy, and sinefungin complexes illustrates that the four  
 256 water molecules occupy analogous positions within the  
 257 substrate binding cleft of the different ligand-bound complexes  
 258 (Figure 1F). Collectively, the structures illustrate that AdoMet,  
 259 AdoHcy, and sinefungin adopt nearly identical conformations  
 260 when bound to the MetH reactivation domain and that water  
 261 molecules serve to bridge the interactions between the AdoMet  
 262 sulfonium cation and Glu1097 and Glu1128 within the  
 263 enzyme's binding cleft.

264 On the basis of our observations in the MetH crystal  
 265 structures, we sought to further examine the water-mediated  
 266 CH···O hydrogen bonding between MetH and the AdoMet  
 267 methyl group in solution. In prior studies with the lysine  
 268 methyltransferase SET7/9, we employed two-dimensional  
 269 heteronuclear single-quantum coherence (2D HSQC) spec-  
 270 troscopy with a <sup>13</sup>C-labeled methyl group of AdoMet (<sup>13</sup>CH<sub>3</sub>-  
 271 AdoMet) to detect CH···O hydrogen bonding between the

substrate's methyl group and residues within the enzyme's  
 272 active site. In the 2D HSQC spectrum of the MetH-<sup>13</sup>CH<sub>3</sub>-  
 273 AdoMet complex, the <sup>1</sup>H chemical shift of the methyl group  
 274 was observed at 3.1 ppm, a 0.1 ppm downfield change  
 275 compared to the reported value of AdoMet free in solution (3.0  
 276 ppm) (Figure 2A).<sup>25</sup> This small alteration in the <sup>1</sup>H chemical  
 277  $\delta$

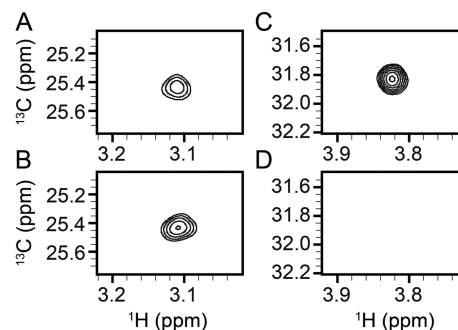
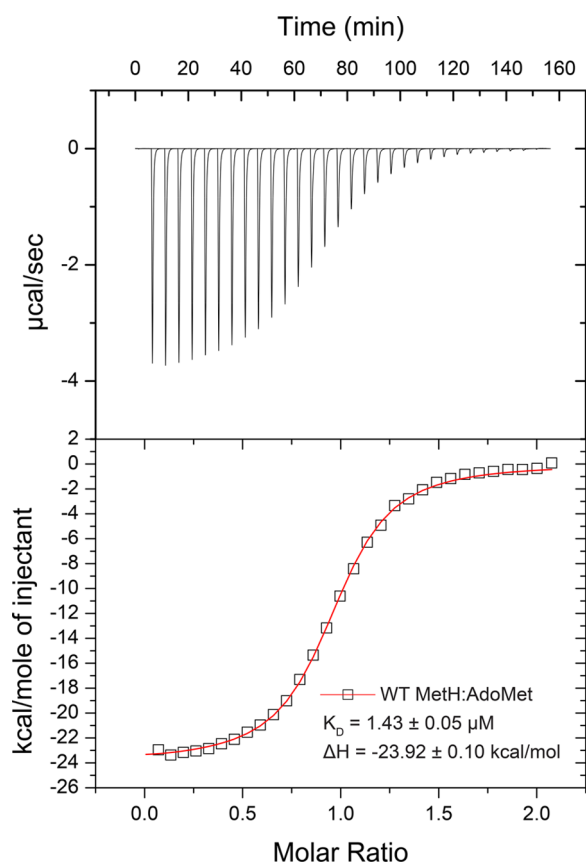


Figure 2. Two-dimensional (A) HSQC and (B) SOFAST-HMQC spectra of the MetH-<sup>13</sup>CH<sub>3</sub>-AdoMet complex and (C) HSQC and (D) SOFAST-HMQC spectra of the SET7/9-<sup>13</sup>CH<sub>3</sub>-AdoMet complex.

shift is consistent with the water-mediated CH···O hydrogen  
 278 bonding of the AdoMet methyl group bound to MetH (Figure  
 279 2A). In contrast, the <sup>1</sup>H chemical shift of <sup>13</sup>CH<sub>3</sub>-AdoMet bound  
 280 to the lysine methyltransferase SET7/9 exhibited a marked  
 281 downfield change of 3.8 ppm (Figure 2B), consistent with  
 282 methyl CH···O hydrogen bonding in the active site, as  
 283 previously reported.<sup>11</sup> As corroboration for these findings, a  
 284 cross-peak was recorded in the band-selective optimized flip  
 285 angle short transient heteronuclear multiple quantum coher-  
 286 ence (SOFAST-HMQC)<sup>26</sup> spectrum of the MetH-<sup>13</sup>CH<sub>3</sub>-  
 287 AdoMet complex, whereas no peak was discernible in the  
 288 spectrum of the SET7/9-<sup>13</sup>CH<sub>3</sub>-AdoMet complex (Figure  
 289 2C,D). The SOFAST-HMQC data concur with the relatively  
 290 solvent-exposed proton rich environment of the AdoMet  
 291 binding cleft in MetH and the general depletion of the  
 292 <sup>1</sup>H-<sup>1</sup>H “relaxation sink” around the substrate's methyl group  
 293 when bound in the active site of SET7/9 (Figure S2).  
 294 Together, the NMR results correlate with the MetH crystal  
 295 structures, illustrating the relative solvent exposure of the  
 296 AdoMet methyl group when bound in the active site.  
 297

Our observations of water-mediated CH···O hydrogen  
 298 bonding between Glu1097 and Glu1128 in MetH and the  
 299 AdoMet sulfonium cation prompted us to examine the  
 300 thermodynamic properties of these interactions and whether  
 301 they contribute to the substrate specificity of the enzyme. Using  
 302 ITC, we measured the equilibrium dissociation constants ( $K_D$ )  
 303 and enthalpies of binding ( $\Delta H$ ) of AdoMet, AdoHcy, and  
 304 sinefungin for the WT enzyme (Figure 3 and Figure S3A,B).  
 305 The ITC data illustrate that the MetH reactivation domain  
 306 bound AdoMet and sinefungin with comparable affinity and  
 307  $\Delta H$  values, whereas it exhibited a 15-fold lower affinity for  
 308 AdoHcy than for AdoMet, with a corresponding decrease in  
 309  $\Delta H$  (Table 1). These results are consistent with the acidic  
 310 surface of the substrate binding cleft and the water-mediated  
 311 hydrogen bonding between the carboxylate anions of Glu1097  
 312 and Glu1128 and the sulfonium and ammonium cations of  
 313 AdoMet and sinefungin, respectively (Figure 1B–D). These  
 314 water-mediated hydrogen bonds would presumably be  
 315 relatively strong because of the positive and negative charges  
 316 of the proton donors and acceptors, respectively. Conversely,  
 317



**Figure 3.** ITC titration of the WT MetH reactivation domain and AdoMet. The top panel shows the titration of AdoMet into the MetH solution, and the bottom panel illustrates the curve fitted to the binding isotherm.

**Table 1.** ITC Data and QM-Calculated Binding Energies ( $E_B$ ) for Ligand Binding by WT MetH and the E1097Q and E1128Q Mutants

	$K_D$ ( $\mu\text{M}$ )					
	WT	E1097Q	E1128Q			
AdoMet	$1.43 \pm 0.05$	$6.10 \pm 0.68$	$17.5 \pm 1.0$			
AdoHcy	$20.8 \pm 0.2$	$15.0 \pm 0.5$	$38.2 \pm 1.0$			
sinefungin	$2.04 \pm 0.07$	$17.7 \pm 1.56$	$44.8 \pm 2.51$			
	$\Delta H$ (kcal mol $^{-1}$ )					
	WT	E1097Q	E1128Q			
AdoMet	$-23.92 \pm 0.10$	$-19.43 \pm 0.16$	$-15.65 \pm 0.09$			
AdoHcy	$-15.30 \pm 0.03$	$-11.95 \pm 0.04$	$-11.22 \pm 0.04$			
sinefungin	$-18.59 \pm 0.09$	$-17.02 \pm 0.17$	$-14.63 \pm 0.13$			
	QM binding energy (kcal mol $^{-1}$ )					
			$\Delta E_B$ [E - Q]		$\Delta E_B$ [E - Q]	
	E1097	Q1097	E1128	Q1128		
MeS $^+$ (Et) $_2$ complex energy	87.69	19.19	68.50	73.41	29.30	44.11
S(Et) $_2$ complex energy	8.45	7.25	1.20	6.30	3.53	2.77
$\Delta E_B$ [MeS $^+$ (Et) $_2$ - S(Et) $_2$ ]	79.24	11.94		67.11	25.77	

AdoHcy would presumably be expected to form weaker water-mediated CH $\cdots$ O hydrogen bonds with the glutamates because of the lack of methyl interactions and its neutral thioester group, consistent with the thermodynamic binding data. To

further probe these findings, we substituted Glu1097 and Glu1128 with glutamine in MetH and examined the effect of these mutations on the binding affinity of the ligands (Figure S3C–H). Glutamine mutations were chosen because of their propensity to weaken the water-mediated hydrogen bonding to the ligands by substituting their side chain carboxylate anions with neutral carboxamide groups, while preserving the hydrogen bonding networks formed by these residues within the active site (Figure S4). The E1097Q and E1128Q mutations diminished the binding affinity of AdoMet and sinefungin from 4- to 22-fold compared to that of WT MetH, whereas binding to AdoHcy was altered by <2-fold. Moreover, each glutamine mutation effectively reduced the difference in the enzyme's binding selectively for AdoMet and AdoHcy to approximately 2-fold. Together, these findings illustrate that the water-mediated CH $\cdots$ O hydrogen bonds formed between the carboxylate groups of Glu1097 and Glu1128 and the AdoMet sulfonium cation are important in conferring recognition of the substrate versus the product and that substitution of these residues with glutamine abrogates this selectively.

To further investigate these findings, we performed quantum mechanical calculations to investigate the CH $\cdots$ O hydrogen bonding between AdoMet and AdoHcy and the glutamates within the MetH substrate binding cleft. To assess the individual contributions of Glu1097 and Glu1128 to AdoMet and AdoHcy recognition, pairwise models of the active site were generated comprising the ligands, each glutamate, and the cognate water molecules that mediate CH $\cdots$ O hydrogen bonding. The active site models were based upon the coordinates of the crystal structures of MetH bound to the substrate and product (Figure 4 and Figure S5). The AdoMet sulfonium cation and AdoHcy thioester were represented as MeS $^+$ (Et) $_2$  and S(Et) $_2$  monomers, respectively, as previously described.<sup>12,27</sup> Glu1097 and Glu1128 were modeled as propionate groups, and the corresponding glutamine substitutions were represented as propionamide moieties using the coordinates of the glutamate side chains, with the carboxamide oxygen atoms oriented toward the ligands to retain an analogous pattern of water-mediated CH $\cdots$ O hydrogen bonding. For the models representing the WT enzyme, the heavy atoms of the ligands and the water molecules were constrained to their crystallographic coordinates, whereas certain carbon atoms in the propionate were constrained to maintain the glutamate side chain conformations observed in the crystal structures. For the propionamide-containing models, the same atoms were held fixed in the ligands and propionamide groups. However, the water molecules were left unrestrained to allow the optimization of their positions relative to the propionamide monomers, with the exception of W4 in the S(Et) $_2$  model that strayed into a position that would sterically clash with atoms in the crystal structures that were not included in the models.

Once the active site models were generated, the binding energy ( $E_B$ ) for each complex was evaluated as the difference in energy between the full complex on one hand and the sum of the ligand and the interacting residue and solvent on the other. We then computed the differences in the  $E_B$  values for the MeS $^+$ (Et) $_2$  and S(Et) $_2$  complexes  $\{\Delta E_B$  [MeS $^+$ (Et) $_2$  - S(Et) $_2$ ]} and the propionate to propionamide substitutions corresponding to the E1097Q and E1128Q mutations ( $\Delta E_B$  [E - Q]) (Table 1). Overall, the trends observed in the  $E_B$  values for the models correlate with the AdoMet and AdoHcy binding affinities and  $\Delta H$  values observed for WT MetH and the

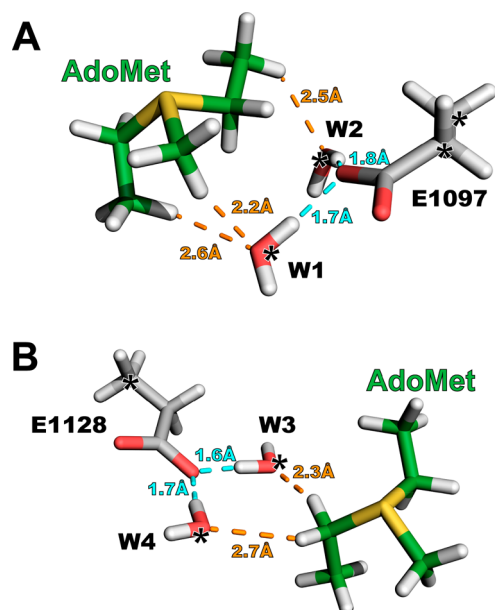


**Figure 4.** Optimized geometry for the minimal active site models used in the QM calculations to determine the binding energies for the (A) AdoMet and Glu1097 and (B) AdoMet and Glu1128 complexes. The AdoMet sulfonium cation was modeled as  $\text{MeS}^+(\text{Et})_2$ , and the glutamate side chains were represented by propionate groups. The ligand heavy atom positions (carbon and sulfur atoms) were constrained to their X-ray coordinates, as were the oxygen atoms in the water molecules and carbon atoms in the propionate monomers that are denoted by asterisks. Conventional and  $\text{CH}\cdots\text{O}$  hydrogen bonds are depicted as cyan and orange dashed lines, respectively, with  $\text{H}\cdots\text{O}$  distances denoted.

385 E1097Q and E1128Q mutants. There is a substantial decrease  
 386 in the  $\Delta E_B$  [ $\text{MeS}^+(\text{Et})_2 - \text{S}(\text{Et})_2$ ] values upon substitution of  
 387 the propionate group with propionamide for both the Glu1097  
 388 and Glu1128 models. This finding is consistent with the ITC  
 389 data illustrating that the differences in the binding affinities for  
 390 AdoMet and AdoHcy are substantially diminished in the  
 391 E1097Q and E1128Q mutants compared to that of WT MetH.  
 392 Correlatively, the values of  $\Delta E_B$  [ $\text{E} - \text{Q}$ ] are substantially larger  
 393 for the  $\text{MeS}^+(\text{Et})_2$  models than for the  $\text{S}(\text{Et})_2$  models for both  
 394 glutamate positions, in agreement with the stronger apparent  
 395 effect of the E1097Q and E1128Q mutants on the binding  
 396 affinities and  $\Delta H$  values for AdoMet than on those of AdoHcy.  
 397 Taken together, the strongest binding energies are observed  
 398 when both the sulfonium cation and carboxylate anions are  
 399 present in the models, whereas the interaction energies are  
 400 diminished upon substitution of neutral thioether or carbox-  
 401 amide groups. These results indicate that the water-mediated  
 402 hydrogen bonding serves as a conduit for the electrostatic  
 403 interactions between the AdoMet sulfonium cation and the  
 404 Glu1097 and Glu1128 carboxylate anions and that the strength  
 405 of these interactions is significantly attenuated when one or  
 406 both ions are substituted by a neutral moiety.

## 407 ■ DISCUSSION

408 Prior studies of different classes of AdoMet-dependent  
 409 methyltransferases have described the presence of  $\text{CH}\cdots\text{O}$   
 410 hydrogen bonding between the AdoMet sulfonium cation and  
 411 residues within the enzymes' active sites.<sup>10</sup> In SET domain  
 412 lysine methyltransferases, these interactions have been shown  
 413 to be important for high-affinity recognition of AdoMet,

enabling these enzymes to distinguish the substrate from the  
 product AdoHcy, thus mitigating product inhibition.<sup>10,27,28</sup> In  
 contrast, the substrate binding cleft of MetH utilizes a different  
 mode of recognition wherein active site glutamates form water-  
 mediated  $\text{CH}\cdots\text{O}$  hydrogen bonds with the AdoMet sulfonium  
 cation. The electrostatic nature of these hydrogen bonds is  
 important, as the removal of one or both charges by glutamate  
 to glutamine mutation or substitution of the AdoMet sulfonium  
 cation by the thioether in AdoHcy diminished the binding  
 affinity,  $\Delta H$  values, and the QM-calculated  $E_B$  values (Table 1).  
 These data suggest a model wherein water-mediated  $\text{CH}\cdots\text{O}$   
 hydrogen bonding between the AdoMet sulfonium cation and  
 acidic residues within the active site of a methyltransferase may  
 serve to enhance substrate recognition. In contrast, water-  
 bridged interactions involving amino acids with neutral polar  
 side chains would potentially form weaker hydrogen bonds that  
 do not contribute to selective AdoMet recognition, consistent  
 with the effect of the glutamate to glutamine substitutions in  
 MetH (Table 1). These findings justify further investigation of  
 how acidic residues may facilitate AdoMet recognition in other  
 methyltransferases.

These results also offer new insights into how the AdoMet/  
 AdoHcy ratio may govern MetH activity in cells. The *E. coli*  
 MetH reactivation domain displayed a 15-fold higher affinity  
 for AdoMet than for AdoHcy (Table 1). This difference in  
 selectivity is achieved in part by water-mediated hydrogen  
 bonding between AdoMet and Glu1097 and Glu1128 in the  
 enzyme. In mammalian MetH, the residue corresponding to  
 Glu1128 in the *E. coli* enzyme is substituted with a leucine.<sup>29</sup>  
 On the basis of the effects of the *E. coli* MetH E1128Q mutant  
 (Table 1), the leucine substitution would presumably weaken  
 its ability to discriminate between AdoMet and AdoHcy,  
 rendering it more susceptible to product inhibition. Mammalian  
 studies investigating AdoMet and AdoHcy concentrations have  
 reported AdoMet/AdoHcy ratios ranging from 2 to 11,  
 depending on the tissue type.<sup>30,31</sup> Metabolic changes that  
 increase the concentration of AdoHcy and decrease the  
 AdoMet/AdoHcy ratio would potentially inhibit the MetH  
 reactivation domain, thus resulting in diminished reactivation  
 of the enzyme with concomitant alterations in the cellular methyl  
 cycle.

Prior studies of a disulfide-stabilized C-terminal construct of  
*E. coli* MetH comprising the cobalamin binding and reactivation  
 domains have revealed that Glu1097 also has a catalytic role in  
 the reactivation cycle.<sup>8,9</sup> The structure of this C-terminal MetH  
 construct bound to cobalamin and AdoHcy illustrates that the  
 side chains of Glu1097 and Tyr1139 form hydrogen bonds to a  
 water molecule coordinated to the Co ion in the cofactor.  
 These interactions stabilize the four-coordinate state of  
 $\text{Co(II)Cbl}$ , promoting the one-electron reduction of  $\text{Co(II)Cbl}$   
 to  $\text{Co(I)Cbl}$ . Structures of the C-terminal construct determined  
 in the absence and presence of AdoHcy indicate that the side  
 chain of Glu1097 undergoes a change in conformation to  
 engage in hydrogen bonding with the Co-coordinated water  
 molecule when AdoHcy is bound, which would also  
 presumably occur when AdoMet is present. Thus, Glu1097,  
 which is invariant in MetH, may serve two functions in the  
 enzyme: (1) to enhance AdoMet binding affinity through  
 water-mediated  $\text{CH}\cdots\text{O}$  hydrogen bonding and (2) to  
 modulate the reduction potential of  $\text{Co(II)Cbl}$  by hydrogen  
 bonding to the Co-bound water molecule.

Finally, our results have important ramifications with respect  
 to the development of AdoMet analogues as competitive

477 inhibitors of methyltransferases. Several of these inhibitors  
478 utilize sinefungin, a natural product pan-methyltransferase  
479 inhibitor, as a scaffold given its isostericity with AdoMet.<sup>32–36</sup>  
480 Given that sinefungin recognizes the MetH reactivation domain  
481 with an affinity comparable to that of AdoMet (Table 1),  
482 analogues derived from it may also bind to the enzyme,  
483 particularly because of the solvent exposure of the substrate  
484 binding cleft that can accommodate chemical derivatizations of  
485 the inhibitor (Figure S2). Sinefungin has been reported to  
486 cause severe nephrotoxicity in mammalian models of  
487 cryptosporidiosis and trypanosomiasis.<sup>37,38</sup> It is conceivable  
488 that this toxicity is due to not only widespread inhibition of  
489 AdoMet-dependent methyltransferases but also abrogation of  
490 MetH reactivation, disrupting methionine biosynthesis and the  
491 cellular methyl cycle. In light of these findings, it would be  
492 advisable that future efforts to devise AdoMet-based inhibitors  
493 of methyltransferases evaluate whether these compounds  
494 inhibit the reactivation domain of MetH to circumvent off-  
495 target effects of these molecules *in vivo*.

## 496 ■ ASSOCIATED CONTENT

### 497 ● Supporting Information

498 The Supporting Information is available free of charge on the  
499 ACS Publications website at DOI: 10.1021/acs.bio-  
500 chem.8b00375.

501 A table reporting the crystallographic and refinement  
502 statistics and figures illustrating the ligand omit maps,  
503 AdoMet binding sites of MetH and SET7/9, ITC data,  
504 and models used for the QM calculations (PDF)

### 505 Accession Codes

506 Coordinates and structure factors for the MetH-AdoMet  
507 (6BM5), MetH-AdoHcy (6BM6), and MetH-sinefungin  
508 (6BDY) complexes have been deposited in the PDB.

## 509 ■ AUTHOR INFORMATION

### 510 Corresponding Author

511 \*Department of Biological Chemistry, University of Michigan,  
512 5301 Medical Science Research Building III, 1150 W. Medical  
513 Center Dr., Ann Arbor, MI 48109. E-mail: rtrievel@umich.edu.  
514 Phone: 734-647-0889. Fax: 734-763-4581.

### 515 ORCID

516 Steve Scheiner: 0000-0003-0793-0369

517 Raymond C. Trievel: 0000-0003-3189-8792

### 518 Funding

519 This work was supported by National Science Foundation  
520 Grant CHE-1508492 to R.C.T.

### 521 Notes

522 The authors declare no competing financial interest.

## 523 ■ ACKNOWLEDGMENTS

524 The authors thank M. Koutmos for providing the cDNA  
525 encoding the *E. coli* MetH reactivation domain and S. Horowitz  
526 for reading the manuscript and furnishing insightful comments  
527 and feedback. This research used resources of the Advanced  
528 Photon Source, a U.S. Department of Energy (DOE) Office of  
529 Science User Facility operated for the DOE Office of Science  
530 by Argonne National Laboratory under Contract DE-AC02-  
531 06CH11357. Use of LS-CAT Sector 21 was supported by the  
532 Michigan Economic Development Corp. and the Michigan  
533 Technology Tri-Corridor (Grant 085P1000817).

## ■ REFERENCES

- 534  
535 (1) Matthews, R. G., Koutmos, M., and Datta, S. (2008) Cobalamin-  
536 dependent and cobamide-dependent methyltransferases. *Curr. Opin.*  
537 *Struct. Biol.* 18, 658–666.  
538 (2) Ludwig, M. L., and Matthews, R. G. (1997) Structure-based  
539 perspectives on B12-dependent enzymes. *Annu. Rev. Biochem.* 66,  
540 269–313.  
541 (3) Banerjee, R. V., and Matthews, R. G. (1990) Cobalamin-  
542 dependent methionine synthase. *FASEB J.* 4, 1450–1459.  
543 (4) Drummond, J. T., Huang, S., Blumenthal, R. M., and Matthews,  
544 R. G. (1993) Assignment of enzymatic function to specific protein  
545 regions of cobalamin-dependent methionine synthase from *Escherichia*  
546 *coli*. *Biochemistry* 32, 9290–9295.  
547 (5) Dixon, M. M., Huang, S., Matthews, R. G., and Ludwig, M.  
548 (1996) The structure of the C-terminal domain of methionine  
549 synthase: Presenting S-adenosylmethionine for reductive methylation  
550 of B-12. *Structure* 4, 1263–1275.  
551 (6) Schubert, H. L., Blumenthal, R. M., and Cheng, X. (2003) Many  
552 paths to methyltransfer: a chronicle of convergence. *Trends Biochem.*  
553 *Sci.* 28, 329–335.  
554 (7) Bandarian, V., Patridge, K. A., Lennon, B. W., Huddler, D. P.,  
555 Matthews, R. G., and Ludwig, M. L. (2002) Domain alternation  
556 switches B(12)-dependent methionine synthase to the activation  
557 conformation. *Nat. Struct. Biol.* 9, 53–56.  
558 (8) Datta, S., Koutmos, M., Patridge, K. A., Ludwig, M. L., and  
559 Matthews, R. G. (2008) A disulfide-stabilized conformer of  
560 methionine synthase reveals an unexpected role for the histidine  
561 ligand of the cobalamin cofactor. *Proc. Natl. Acad. Sci. U. S. A.* 105,  
562 4115–4120.  
563 (9) Koutmos, M., Datta, S., Patridge, K. A., Smith, J. L., and  
564 Matthews, R. G. (2009) Insights into the reactivation of cobalamin-  
565 dependent methionine synthase. *Proc. Natl. Acad. Sci. U. S. A.* 106,  
566 18527–18532.  
567 (10) Horowitz, S., Dirk, L. M., Yesselman, J. D., Nimtz, J. S.,  
568 Adhikari, U., Mehl, R. A., Scheiner, S., Houtz, R. L., Al-Hashimi, H. M.,  
569 and Trievel, R. C. (2013) Conservation and functional importance of  
570 carbon-oxygen hydrogen bonding in AdoMet-dependent methyltrans-  
571 ferases. *J. Am. Chem. Soc.* 135, 15536–15548.  
572 (11) Horowitz, S., Yesselman, J. D., Al-Hashimi, H. M., and Trievel,  
573 R. C. (2011) Direct evidence for methyl group coordination by  
574 carbon-oxygen hydrogen bonds in the lysine methyltransferase SET7/  
575 9. *J. Biol. Chem.* 286, 18658–18663.  
576 (12) Fick, R. J., Kroner, G. M., Nepal, B., Magnani, R., Horowitz, S.,  
577 Houtz, R. L., Scheiner, S., and Trievel, R. C. (2016) Sulfur-Oxygen  
578 Chalcogen Bonding Mediates AdoMet Recognition in the Lysine  
579 Methyltransferase SET7/9. *ACS Chem. Biol.* 11, 748–754.  
580 (13) Otwinowski, Z., and Minor, W. (1997) Processing of X-ray  
581 diffraction data collected in oscillation mode. *Methods Enzymol.* 276,  
582 307–326.  
583 (14) McCoy, A. J., Grosse-Kunstleve, R. W., Adams, P. D., Winn, M.  
584 D., Storoni, L. C., and Read, R. J. (2007) Phaser crystallographic  
585 software. *J. Appl. Crystallogr.* 40, 658–674.  
586 (15) Emsley, P., and Cowtan, K. (2004) Coot: model-building tools  
587 for molecular graphics. *Acta Crystallogr., Sect. D: Biol. Crystallogr.* 60,  
588 2126–2132.  
589 (16) Emsley, P., Lohkamp, B., Scott, W. G., and Cowtan, K. (2010)  
590 Features and development of Coot. *Acta Crystallogr., Sect. D: Biol.*  
591 *Crystallogr.* 66, 486–501.  
592 (17) Adams, P. D., Afonine, P. V., Bunkoczi, G., Chen, V. B., Davis, I.  
593 W., Echols, N., Headd, J. J., Hung, L. W., Kapral, G. J., Grosse-  
594 Kunstleve, R. W., McCoy, A. J., Moriarty, N. W., Oeffner, R., Read, R.  
595 J., Richardson, D. C., Richardson, J. S., Terwilliger, T. C., and Zwart, P.  
596 H. (2010) PHENIX: a comprehensive Python-based system for  
597 macromolecular structure solution. *Acta Crystallogr., Sect. D: Biol.*  
598 *Crystallogr.* 66, 213–221.  
599 (18) Baker, N. A., Sept, D., Joseph, S., Holst, M. J., and McCammon,  
600 J. A. (2001) Electrostatics of nanosystems: application to microtubules  
601 and the ribosome. *Proc. Natl. Acad. Sci. U. S. A.* 98, 10037–10041.

- 602 (19) Goddard, T. G., and Kneller, D. G. SPARKY 3, University of  
603 California, San Francisco.
- 604 (20) Delaglio, F., Grzesiek, S., Vuister, G. W., Zhu, G., Pfeifer, J., and  
605 Bax, A. (1995) NMRPipe - a Multidimensional Spectral Processing  
606 System Based on Unix Pipes. *J. Biomol. NMR* 6, 277–293.
- 607 (21) Frisch, M. J., Trucks, G. W., Schlegel, H. B., Scuseria, G. E.,  
608 Robb, M. A., Cheeseman, J. R., Scalmani, G., Barone, V., Mennucci, B.,  
609 Petersson, G. A., Nakatsuji, H., Caricato, M., Li, X., Hratchian, H. P.,  
610 Izmaylov, A. F., Bloino, J., Zheng, G., Sonnenberg, J. L., Hada, M.,  
611 Ehara, M., Toyota, K., Fukuda, R., Hasegawa, J., Ishida, M., Nakajima,  
612 T., Honda, Y., Kitao, O., Nakai, H., Vreven, T., Montgomery, J. A., Jr.,  
613 Peralta, J. E., Ogliaro, F., Bearpark, M., Heyd, J. J., Brothers, E., Kudin,  
614 K. N., Staroverov, V. N., Kobayashi, R., Normand, J., Raghavachari, K.,  
615 Rendell, A., Burant, J. C., Iyengar, S. S., Tomasi, J., Cossi, M., Rega, N.,  
616 Millam, J. M., Klene, M., Knox, J. E., Cross, J. B., Bakken, V., Adamo,  
617 C., Jaramillo, J., Gomperts, R., Stratmann, R. E., Yazyev, O., Austin, A.  
618 J., Cammi, R., Pomelli, C., Ochterski, J. W., Martin, R. L., Morokuma,  
619 K., Zakrzewski, V. G., Voth, G. A., Salvador, P., Dannenberg, J. J.,  
620 Dapprich, S., Daniels, A. D., Farkas, O., Foresman, J. B., Ortiz, J. V.,  
621 Cioslowski, J., and Fox, D. J. (2009) *Gaussian 09*, revision B.01,  
622 Gaussian, Inc., Wallingford, CT.
- 623 (22) Zhao, Y., and Truhlar, D. G. (2008) The M06 suite of density  
624 functionals for main group thermochemistry, thermochemical kinetics,  
625 noncovalent interactions, excited states, and transition elements: two  
626 new functionals and systematic testing of four M06-class functionals  
627 and 12 other functionals. *Theor. Chem. Acc.* 120, 215–241.
- 628 (23) Barone, V., and Cossi, M. (1998) Quantum calculation of  
629 molecular energies and energy gradients in solution by a conductor  
630 solvent model. *J. Phys. Chem. A* 102, 1995–2001.
- 631 (24) Adhikari, U., and Scheiner, S. (2013) Magnitude and  
632 mechanism of charge enhancement of CH••O hydrogen bonds. *J.*  
633 *Phys. Chem. A* 117, 10551–10562.
- 634 (25) Seeger, K., Lein, S., Reuter, G., and Berger, S. (2005) Saturation  
635 transfer difference measurements with SU(VAR)3–9 and S-adenosyl-  
636 L-methionine. *Biochemistry* 44, 6208–6213.
- 637 (26) Schanda, P., Kupce, E., and Brutscher, B. (2005) SOFAST-  
638 HMQC experiments for recording two-dimensional heteronuclear  
639 correlation spectra of proteins within a few seconds. *J. Biomol. NMR*  
640 33, 199–211.
- 641 (27) Horowitz, S., Adhikari, U., Dirk, L. M., Del Rizzo, P. A., Mehl, R.  
642 A., Houtz, R. L., Al-Hashimi, H. M., Scheiner, S., and Trievel, R. C.  
643 (2014) Manipulating unconventional CH-based hydrogen bonding in  
644 a methyltransferase via noncanonical amino acid mutagenesis. *ACS*  
645 *Chem. Biol.* 9, 1692–1697.
- 646 (28) Couture, J. F., Hauk, G., Thompson, M. J., Blackburn, G. M.,  
647 and Trievel, R. C. (2006) Catalytic roles for carbon-oxygen hydrogen  
648 bonding in SET domain lysine methyltransferases. *J. Biol. Chem.* 281,  
649 19280–19287.
- 650 (29) Wolthers, K. R., Toogood, H. S., Jowitt, T. A., Marshall, K. R.,  
651 Leys, D., and Scrutton, N. S. (2007) Crystal structure and solution  
652 characterization of the activation domain of human methionine  
653 synthase. *FEBS J.* 274, 738–750.
- 654 (30) Caudill, M. A., Wang, J. C., Melnyk, S., Pogribny, I. P., Jernigan,  
655 S., Collins, M. D., Santos-Guzman, J., Swendseid, M. E., Cogger, E. A.,  
656 and James, S. J. (2001) Intracellular S-adenosylhomocysteine  
657 concentrations predict global DNA hypomethylation in tissues of  
658 methyl-deficient cystathionine beta-synthase heterozygous mice. *J.*  
659 *Nutr.* 131, 2811–2818.
- 660 (31) Smith, D. E., Hornstra, J. M., Kok, R. M., Blom, H. J., and  
661 Smulders, Y. M. (2013) Folic acid supplementation does not reduce  
662 intracellular homocysteine, and may disturb intracellular one-carbon  
663 metabolism. *Clin. Chem. Lab. Med.* 51, 1643–1650.
- 664 (32) Cai, X. C., Kapilashrami, K., and Luo, M. (2016) Synthesis and  
665 Assays of Inhibitors of Methyltransferases. *Methods Enzymol.* 574,  
666 245–308.
- 667 (33) Tisi, D., Chiarparin, E., Tamanini, E., Pathuri, P., Coyle, J. E.,  
668 Hold, A., Holding, F. P., Amin, N., Martin, A. C., Rich, S. J., Berdini,  
669 V., Yon, J., Acklam, P., Burke, R., Drouin, L., Harmer, J. E., Jeganathan,  
670 F., van Montfort, R. L., Newbatt, Y., Tortorici, M., Westlake, M.,  
Wood, A., Hoelder, S., and Heightman, T. D. (2016) Structure of the  
Epigenetic Oncogene MMSET and Inhibition by N-Alkyl Sinefungin  
Derivatives. *ACS Chem. Biol.* 11, 3093–3105.
- (34) Devkota, K., Lohse, B., Liu, Q., Wang, M. W., Staerk, D.,  
Berthelsen, J., and Clausen, R. P. (2014) Analogues of the Natural  
Product Sinefungin as Inhibitors of EHMT1 and EHMT2. *ACS Med.*  
*Chem. Lett.* 5, 293–297.
- (35) Liu, Q., Cai, X., Yang, D., Chen, Y., Wang, Y., Shao, L., and  
Wang, M. W. (2017) Cycloalkane analogues of sinefungin as EHMT1/  
2 inhibitors. *Bioorg. Med. Chem.* 25, 4579–4594.
- (36) Zheng, W., Ibanez, G., Wu, H., Blum, G., Zeng, H., Dong, A., Li,  
F., Hajian, T., Allali-Hassani, A., Amaya, M. F., Siarheyeva, A., Yu, W.,  
Brown, P. J., Schapira, M., Vedadi, M., Min, J., and Luo, M. (2012)  
Sinefungin derivatives as inhibitors and structure probes of protein  
lysine methyltransferase SETD2. *J. Am. Chem. Soc.* 134, 18004–18014.
- (37) Zweggarth, E., Schillinger, D., Kaufmann, W., and Rottcher, D.  
(1986) Evaluation of sinefungin for the treatment of Trypanosoma  
(Nannomonas) congolense infections in goats. *Trop. Med. Parasitol.*  
37, 255–257.
- (38) Kalimoutou, S., Skiba, M., Bon, P., Dechelotte, P., Arnaud, P.,  
and Lahiani-Skiba, M. (2009) Sinefungin-PLGA nanoparticles: drug  
loading, characterization, in vitro drug release and in vivo studies. *J.*  
*Nanosci. Nanotechnol.* 9, 150–158.